



(Peer Reviewed, Refereed and Multidisciplinary Journal)

Universal Research and Academic Journal

Volume: 03, Issue: 03, (March-2026), pp: 01-12

Received: 10th March, 2026

Accepted: 18th March, 2026

©URAJ: 2026/03/001/012/001

A Study on the Simplified Equation for the Young's Modulus of Concrete Reinforced Using Carbon Nanotubes (CNT)

Nakul Misra¹, Dr. Gaurav Shukla²

¹Research Scholar, Department of Civil Engineering, School of Engineering & Technology, Maharishi University of Information Technology, Lucknow, Uttar Pradesh (esotericnakul@gmail.com)

²Assistant Professor, Department of Civil Engineering, School of Engineering & Technology, Maharishi University of Information Technology, Lucknow, Uttar Pradesh (gaur.knit@gmail.com)

Abstract: This research study examines finite element modeling of Carbon Nanotube (CNT) reinforced concrete matrices for three concrete grades: M40, M60, and M120. A Representative Volume Element (RVE) was utilized, and a one-eighth model of the CNT-reinforced concrete matrix was simulated using the finite element analysis (FEA) software ANSYS. Finite element modeling simulations accurately duplicated the CNT reinforced concrete matrix by adopting random orientations of CNTs with nine fiber volume fractions ranging from 0.1% to 0.9%. The longitudinal and transverse Young's modulus of elasticity of the CNT reinforced concrete was determined by model evaluations. The graphical representations of different fiber volume fractions and concrete grades provided a simplified equation for determining Young's modulus. It also capitalized on the observation that the concrete grade does not substantially influence the CNT reinforced concrete matrix. Results demonstrate that the inclusion of CNT enhances the stiffness of concrete, with the new equation strongly correlating with empirical results.

Keywords: Carbon Nanotubes (CNT), Concrete, Elastic modulus, Representative Volume Element (RVE), Reinforced Concrete

Introduction: Since their invention by Iijima S. in 1991, carbon nanotubes (CNTs) have gained extensive utilization and acceptance on a global scale^[1]. The seamless tubes of the 21st century exhibit exceptionally high mechanical properties and find applications across electronics, biology, chemistry, and multifunctional composites. The carbon nanotubes (CNTs) consist of rolled graphene sheets that exhibit remarkable theoretical strength, approximately 100 times greater than that of steel. Their specific gravity is one-sixth that of steel, with an elastic strain of 12%, a Young's modulus of 1 TPa, and a tensile strength of 200 GPa^[2]. The Carbon nanotubes (CNTs) have a remarkable ability to enhance the mechanical properties of whatever material they are used with. By following the law of mixing, the tensile and flexural strengths of the cement composites were achieved^[3]. According to Rouiania et al., previous studies on CNT reinforced concrete have relied on the nonlinearity of the concrete and the presence of interfacial bonding to derive the constitutive relations, which in turn require that the CNTs are uniformly distributed and have a unidirectional orientation inside the cement matrix^[4]. Hasan et al. assumed a random distribution of nanotubes in cement and derived a new factor proposed for the random orientation of CNT in the cement matrix. The results of analytical modeling demonstrated a strong correlation with the experimental data. The scientist established a distribution function for

fibre orientation within the composite, and the effective mechanical properties of the fibres were calculated according to their position angle in the composite. The random orientation of the fibers diminished the impact of fiber reinforcement compared to unidirectional orientation. An analytical model to predict the compressive strength of CNT/cement composite was derived using the representative elementary volume (REV) method.

Several analytical models were predicated on a unit cell featuring singular fiber reinforcement. The various modeling methodologies utilized finite element modeling (FEM), treating the carbon nanotubes (CNTs) as line elements, hollow cylinders, and solid cylinders. The arrangement of fibers was observed to adhere to a certain principle in the matrix reinforced with CNTs. Mavalizadeh et al. utilized the representative elementary volume (REV) method and finite element method (FEM) to investigate the influence of matrix volume fraction on the transverse Young's modulus. They demonstrated that for both hollow and filled single-walled carbon nanotubes (SWNTs), the effective Young's modulus of the model decreases approximately linearly with an increase in matrix volume fraction^[5]. The primary problem in the CNT-reinforced concrete matrix is the effective dispersion of agglomerated nanotubes. Numerous approaches have been

developed, including the innovative WS2 nano-reinforced cement, which demonstrated that the tensile, flexural, and fracture toughness properties of concrete can be enhanced by the use of nanomaterials^[6]. Studies have demonstrated that the addition of lower concentrations of either carbon nanotubes (CNTs) or carbon nanofibers (CNFs) can enhance strength, ductility, and fracture toughness. The transition to fibre reinforced concrete (FRC) is supported by evidence that individual fibres can enhance tensile strength more effectively than a limited number of steel pieces^[7].

This low percentile sufficiently improves the compressive, tensile, and flexural strength of the cement matrix^[8]. A substantial body of research exists on CNT reinforcement and dispersion, with studies utilizing both Single-Walled Carbon Nanotubes (SWNTs) and Multi-Walled Carbon Nanotubes (MWNTs) in concentrations ranging from 0.01% to 2%^[9]. Studies involving macroscopic scale treat embedding the CNTs as reinforcement in appropriate volume percentage. In order to accurately describe the concrete composites, the matrix had been simulated using a number of different nonlinear constitutive models. The concept of complete bonding between carbon nanotubes (CNTs) and matrix in continuum mechanics has been developed after a variety of experiments at the mesoscopic scale exhibiting the

structural morphology of carbon nanotube (CNT) reinforcements. According to the findings of the nano indentation experiment, MWCNTs have the ability to significantly strengthen the cement paste matrix at the nano scale, which results in an increase in the quantity of high-strength C-S-H gel and a decrease in porosity. It is anticipated that the surface-modified nanotubes and CSH crystals will provide a high binding strength, which will ultimately result in load transfer from the cement matrix to the reinforcement^[10].

The numerical investigations demonstrated that the meshless approach, experiments, and the finite element model for random distribution with high CNT concentration were all in good agreement with one another^[11]. C. Ramesh Babu proposed the utilization of carbon nanotubes as reinforcement bars and fibers within a concrete matrix. This study investigates the application of carbon nanotubes, both single-walled and multi-walled, as fiber reinforcements across various fiber volume fractions, ranging from 0.1% to 1.0%. The analysis employs the representative volume element method (RVE) using finite element analysis (FEA) software ANSYS, culminating in a simplified equation for calculating the Young's modulus of a concrete matrix reinforced with carbon Nanotubes^[12].

(A) Carbon Nanotube (CNTs) Synthesis and Concrete Bonding:

In contrast to MWNTs, whose diameters can be 2–100 nm or even more, SWNTs are typically between 0.5 and 4 nm in size. It is possible to create carbon nanotubes (CNTs) from carbon-based materials and sources. ARC discharge, laser ablation, and chemical vapour deposition (CVD) are the three most popular techniques^[13].

The initial two methods were previously employed in the production of single-walled carbon nanotubes (SWNTs), while chemical vapor deposition is associated with the synthesis of multi-walled carbon nanotubes (MWNTs). The synthesis of carbon nanotubes (CNTs) presents significant challenges due to the necessity of purification methods to remove amorphous carbon, catalysts, and other residual impurities. However, these actions are removed in chemical vapor deposition (CVD). The CVD process presents a limitation in that it requires the preparation and calcination of catalysts for the growth of CNTs. The challenge in the bonding between CNTs and the concrete matrix, particularly regarding the interfacial relationship, is identified as a grey area by Nagesh et al. The agglomeration of CNTs hinders their uniform dispersion within the binder matrix, thereby impacting the overall homogenization. Aqueous solutions utilizing surfactants as dispersants have addressed this issue. Surfactants in larger volumes may impede the hydration process of cement. The

CNTs function as nano-fillers, facilitating hydration by promoting the formation of CSH gel, provided that agglomeration is mitigated. The presence of CNTs would enhance the nucleation and surface area of the CSH gel^[14].

(B) Determine Young's Modulus of Randomly Oriented CNT Reinforced Concrete:

Drugan and Willis project the Representative Elementary Volume (REV) is defined as the minimal volume that accurately represents a composite material with spatially uniform macroscopic constitutive properties, ensuring sufficient accuracy for constitutive relations and responses. To substitute a heterogeneous material with a homogeneous one, the underlying assumptions include that the chosen volume must be sufficiently large to represent the microstructure while remaining small enough for analytical analysis. The representative elementary volume (REV) would maintain equivalent elastic constants and fiber volume fractions as those present in the composite material. This study has identified the REV by incorporating hollow CNTs without additional e-materials in the concrete matrix for fiber volume fractions ranging from 0.1% to 0.90%. The finite element model created illustrated the random distribution of carbon nanotubes (CNTs), simulating the orientation of structural elements composed of concrete, regardless of whether they are reinforced or

unreinforced with steel bars. This method is employed for the representative elementary volume^[15].

The elastic properties of composites can be expressed in terms of Young's modulus (E), shear modulus (G), and Poisson's ratio (μ). The heterogeneous composites necessitate extensive material properties, and the experimental determination of these properties is both labor-intensive and costly. Analytical homogenization may serve as an alternative to experimentation.

The analytical models would exhibit significant variation, demonstrating both complexity and accuracy. The stiffness tensor U and compliance tensor Z of the composites are-

$$U = \sum T_i U^i R^i; \sum T_i R^i = I; z = \sum T_i Z_i B^i \text{ and } \sum T_i B^i = I \quad (i)$$

In this context, T_i , U_i , and Z_i represent the volume fraction, stiffness, and compliance tensors of the i th phase of the composite, respectively, while I denotes the 6 x 6 identity matrix. R_i and B_i represent the strain and stress concentration tensors for the i -th phase, respectively. In fiber-reinforced composites, $I = f, m$ denotes the fiber and matrix phases, respectively. In composites with random fiber orientation, the stiffness tensor exhibits transverse isotropy. This type of transversely isotropic material possesses a single

axis of symmetry. It is characterized by five constants. Barbero proposes three potential representative volume elements (RVE) for a composite material characterized by a periodic, square fiber array, as illustrated in figure (i).

$$D_{11} = \lambda_m + 2\mu_m - \frac{V_f}{J} \left[\frac{A_3^2}{\mu_m^2} - \frac{2A_6 A_3}{g\mu_m^2} - \frac{aA_3}{\mu_m c} + \frac{A_6^2 - A_7^2}{g^2 \mu_m^2} - \frac{A_6 a + A_7 b}{\mu_m c g} + \frac{a^2 - b^2}{4c^2} \right] \quad (ii)$$

$$D_{23} = \lambda_m + \frac{V_f}{J} \left[\frac{A_3}{2\mu_m c} - \frac{A_6 - A_7}{2\mu_m c g} - \frac{a+b}{4c^2} \right] \quad (iii)$$

$$D_{22} = \lambda_m - 2\mu_m - \frac{V_f}{J} \left[\frac{aA_3}{2\mu_m c} + \frac{aA_6}{2\mu_m c g} - \frac{a^2 - b^2}{4c^2} \right] \quad (iv)$$

$$D_{44} = \mu_m - V_f \left[-2 \frac{A_3}{\mu_m} + (\mu_m - \mu_f)^{-1} + \frac{4A_7}{\mu_m(2-2\mu_m)} \right]^{-1} \quad (v)$$

$$D_{66} = \mu_m - V_f \left[-\frac{A_3}{\mu_m} + (\mu_m - \mu_f)^{-1} \right]^{-1} \quad (vi)$$

$$J = \frac{aA_3^2}{2\mu^2 m^c} - \frac{aA_6 A_3}{g\mu_m^2} + \frac{a(A_6^2 - A_7^2)}{2cg^2 \mu_m^2} + \frac{A_3(b^2 - a^2)}{2\mu_m c^2} + \frac{A_6(a^2 - b^2) + A_7(ab^2 + b^2)}{2\mu_m c^2 g} + \frac{(a^3 - 2b^3 - 3ab^2)}{8c^3} \quad (vii)$$

The composite with a periodic microstructure can be represented by Fourier series to assess all components of the stiffness tensor for the specific composite. Barbero posits that composites with randomly oriented fibers exhibit transversely isotropic properties, resulting in a microstructure

characterized by square symmetry. Consequently, the stiffness tensor is defined by six unique coefficients, as delineated by the following six equations.

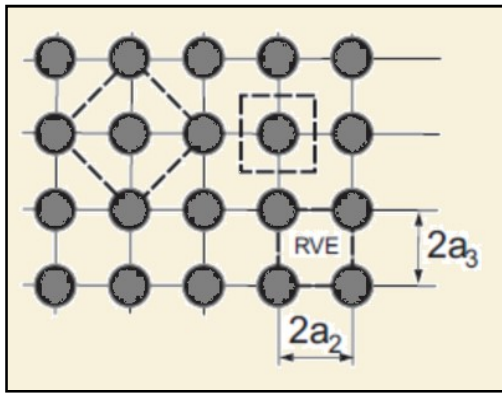


Figure: 1 shows of the three Possible Representative Elementary Volume (RVE)

According to Barbero, the constants a_2 and a_3 should be set at equal intervals in a square array along the x-axis for composites reinforced with cylindrical, long, and circular fibers.

$$A_3 = 0.49 - 0.47V_f - 0.02V_f^2 \tag{viii}$$

$$A_6 = 0.368 - 0.14V_f - 0.027V_f^2 \tag{ix}$$

$$A_7 = 0.12 - 0.32V_f + 0.23V_f^2 \tag{x}$$

Because of the periodic design, the resultant tensor A^* would look like a square array. The transversely isotropic stiffness tensor derives from the random fiber orientation in most composites, and the independent constants for this tensor are 5. By utilizing the coefficients of the tensor A^* , one

may determine the values of the shear modulus G and Young's modulus of elasticity E . Since it is usually not feasible to ensure that the fibers in a concrete matrix are all oriented uniformly, the random microstructure is expected to produce transversely isotropic properties at the mesoscale.

(C) Modeling Using Finite Elements:

The finite element modeling was derived from the work of Barbero et al. on computational micromechanics. The representative volume element (RVE) with dimensions $2a_1 \times 2a_2 \times 2a_3$ was selected for the analysis, and 1/8th of the RVE was simulated using ANSYS, as illustrated in figure 2 below. The mesh volume consists of a maximum of 172 elements and 330 nodes. This simulation facilitated precise replication of the CNT reinforced concrete matrix, incorporating random orientation across various types of concrete, including NSC, HSC, and UHSC. The nanotubes exhibited a hollow structure and were arranged without the presence of any additional material. The volume fractions were determined based on the volume of the concrete matrix.

The designation $2a_1$ is oriented in the z direction, $2a_2$ is oriented in the x direction, and $2a_3$ is oriented in the y direction. The boundary conditions were established as $x=y=z=0$. Subsequently, a uniform displacement is applied in the z direction. The specified boundary

conditions revealed that the FEA model and its components exhibit macroscopic orthotropy. The SOLID 65 element was utilized to model the concrete matrix, accompanied by a random orientation of carbon nanotubes (CNTs) for different fiber volume fractions ranging from 0.1% to 0.9%. The simulated model is capable of predicting the Young's modulus of the CNT reinforced concrete matrix in both the transverse and longitudinal directions, as well as the Poisson ratio of the composite and the shear moduli. With a young's modulus of 1TPa and a Poisson's ratio of 0.22, the single-walled carbon nanotubes (SWNTs) were presumed to have a diameter of 3nm. The 100-nm-diameter MWNTs (multi-walled carbon nanotubes) exhibited the same characteristic. Figure 2 shows the ANSYS, finite element model of the simulated volume at the 1/8 scale. Different grades of concrete were available, with normal strength ranging from 40 MPa, high strength from 60 MPa, and ultra high strength from 120 MPa.

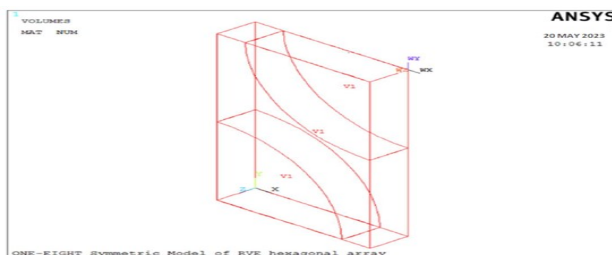


Figure: 2 shows a one-eighth symmetric representation of the representative volume element (RVE) in a hexagonal array

Figure 3 shows the representative volume subsequent to meshing. The boundary conditions stipulated that $x = y = 0$, with displacement applied in the z direction, resulting in $z = a_1$. The stress boundary conditions were implemented to ensure that all constituents and the matrix exhibit macroscopic orthotropy. The analysis produced Young's modulus in the longitudinal direction (EL) and transverse direction (ET), the Poisson's ratio (μ), shear modulus (G), and associated coefficients.

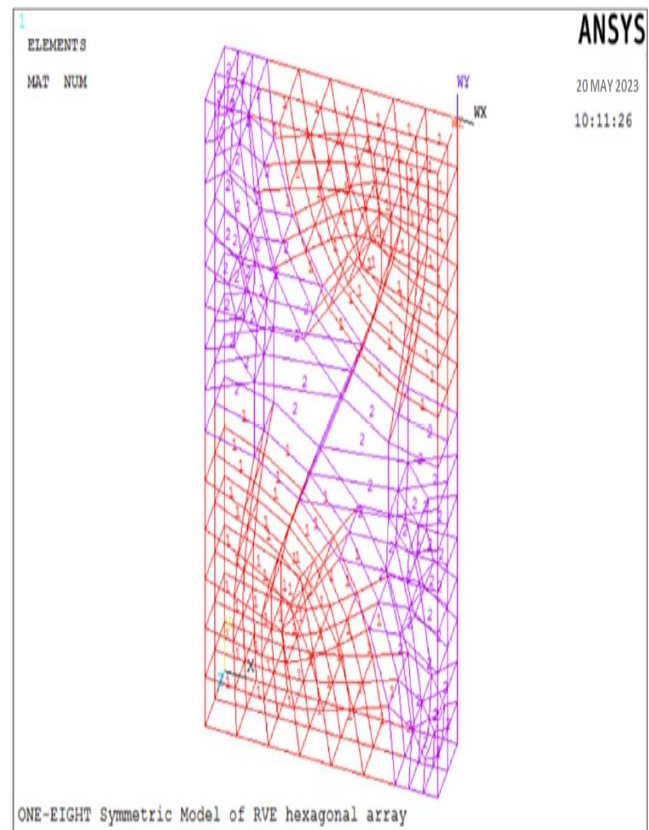


Figure 3 shows the meshed representative volume of the concrete matrix incorporating fibers

Results and Discussions:

Finite element analysis indicated that a finite element model representing 1/8th of the volume element was utilized to determine the longitudinal Young’s modulus of elasticity for the SWNT and MWNT reinforced concrete matrix. The curves presented in figures 4 to 6 shows the relationship between fiber volume fraction and Young's modulus in both the longitudinal and transverse directions. The finite element model achieved convergence at 0.9%, leading to the termination of further analysis. The longitudinal modulus of elasticity (EL) for Single-Walled Carbon Nanotubes (SWNT) and Multi-Walled Carbon Nanotubes (MWNT) exhibited a linear relationship, as demonstrated in the figures 4 and 5.

The observed trend for both types of CNTs showed minimal difference. Nonlinear variation was observed in curves 6 and 7, which illustrate the relationship between fibre volume fraction and the transverse Young’s modulus of elasticity (ET) for SWNT or MWNT reinforced concrete matrix. The curves were generated for three grades of concrete, encompassing a broad spectrum from normal strength concrete to ultra-high strength concrete. The characteristic compressive strengths of 40 MPa, 60 MPa, and 120 MPa were utilized in this investigation. The graphical plots indicate that

the concrete grade does not significantly impact strength enhancement.

Additionally, a low dosage of CNTs is sufficient to exert a notable influence on CNT reinforced concrete composites. Utilizing the finite element model and representative volume element, the subsequent equations have been derived for EL and ET across three concrete grades. In evaluating the Young’s modulus of elasticity in the transverse direction, Single-Walled Nanotubes (Swnts) demonstrate a positive contribution to the strength enhancement of the concrete matrix. A decrease in transverse Young’s modulus was noted for the Multi-Walled Carbon Nanotubes (Mwnts). The equations presented above represent the Young’s modulus of elasticity for CNT reinforced concrete, measured in both transverse and longitudinal directions, expressed in gigapascals (GPa). The analysis of regression indicated an observed R2 value of 1 across all derived equations for Young’s modulus of elasticity, as shown in Table 1 and 2.

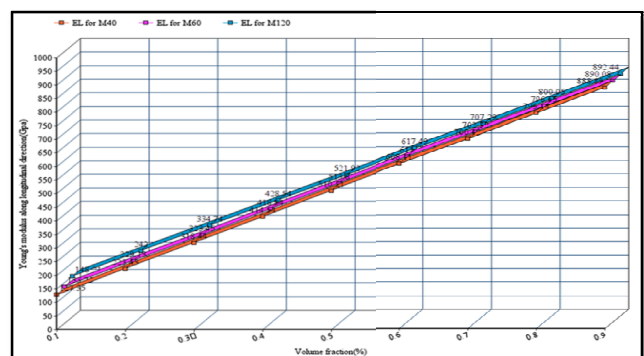


Figure: 4 shows the relationship between the fibre volume fraction and electrical conductivity for Single-Walled Carbon Nanotubes (SWNT)

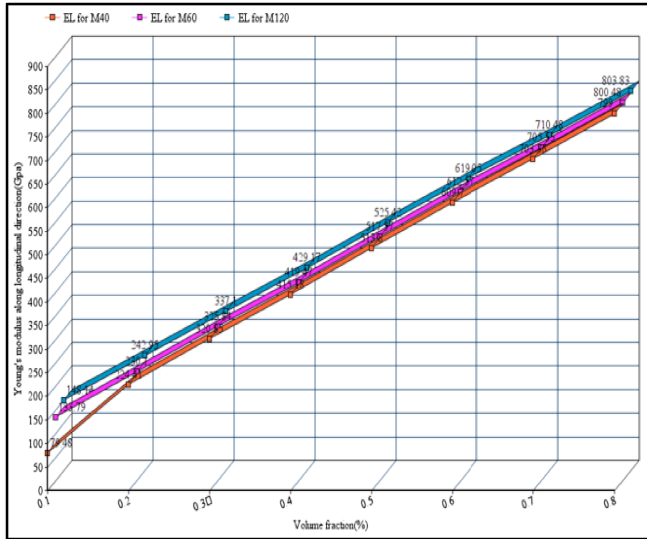


Figure: 5 shows the relationship between the fibre volume fraction and electrical conductivity for Multi-Walled Carbon Nanotubes (MWNT)

The impact of unconfined concrete strength, the observations from figures 4 to 7 indicate a positive correlation between the fibre volume fraction and the Young’s modulus of elasticity of concrete. The variations exhibit linear characteristics in the case of the longitudinal modulus of elasticity EL, while the transverse Young’s modulus of elasticity ET demonstrates a nonlinear variation. Figure 4 shows that for all grades of concrete, specifically M40, M60, and M120, the longitudinal Young's modulus of elasticity exhibited an incremental value of 0.125% for SWNT. The percentile value for the longitudinal Young's modulus of MWNT

was approximately 0.18%, as can be confirmed by referring to Figure 5.

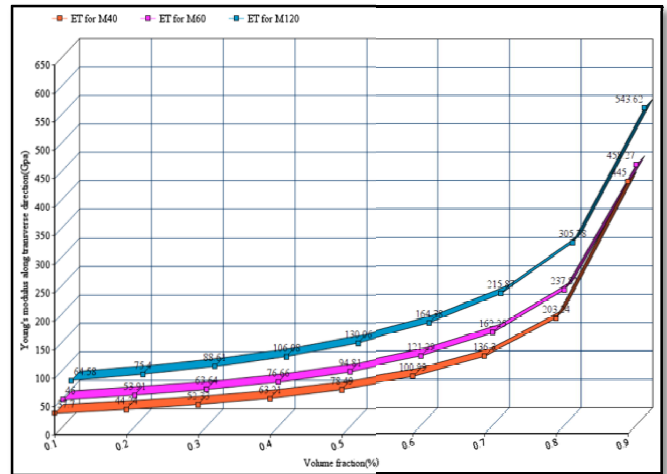


Figure: 6 shows the relationship between the fibre volume fraction and the Electrical Transport (ET) for Single-Walled Carbon Nanotubes (SWNT)

Single-Walled Carbon Nanotubes (SWNT)			
	M40	M60	M120
E_L	935(V_f) + 33.06	946.29(V_f) + 40.08	930.93(V_f) + 56
E_T	1015(V_f) ² - 629.58(V_f) + 122.46	1050.77(V_f) ² - 629(V_f) + 130	1089.93(V_f) ² - 602(V_f) + 144.57

Multi-Walled Carbon Nanotubes (MWNT)			
	M40	M60	M120
E_L	1073(V_f) 1.07	948.12(V_f) 0.87	935.34(V_f) 0.82

E_T	$417.9(V_f) 2$	$486.2(V_f)2$	$579.1(V_f) 2 -$
	$- 157.9(V_f)$	$- 186.2(V_f)$	$201.6(V_f) +$
	$+ 54.4$	$+ 67.7$	88

Table: 1 and 2 shows the equations for determining Young's modulus of CNT-Reinforced Concrete

The variations exhibited a linear pattern. Further observations from figures 6 and 7 reveal a nonlinear variation in the case of ET, with an observed increase of approximately 2.24% in the transverse Young's modulus for any grade of concrete. The data indicate that concrete strength does not significantly affect Young's modulus of elasticity in either the longitudinal or transverse direction.

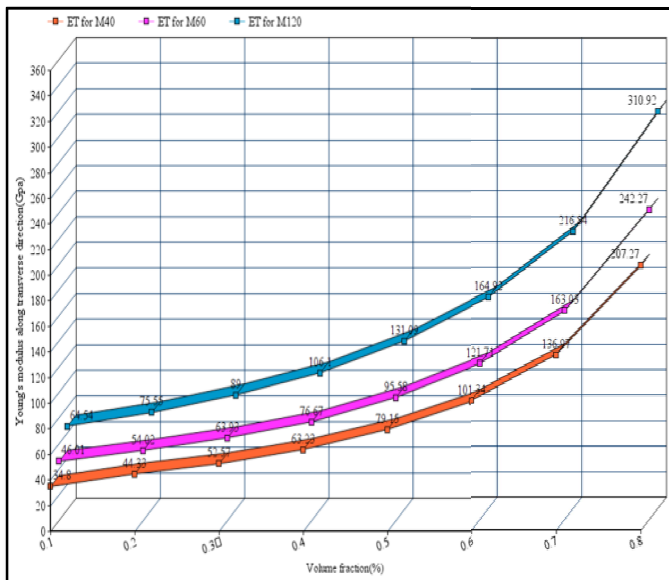


Figure: 7 shows the relationship between fibre volume fraction and ET MWNT

The fibre volume fraction significantly affects both the longitudinal and transverse Young's modulus of elasticity, as evidenced by the data presented in Figures 4 to 7. A linear variation indicated an enhancement of approximately 47% in the longitudinal Young's modulus of elasticity (EL) as shown in plots 4 and 5. An exponential variation in the transverse Young's modulus of elasticity (ET) was observed, as illustrated in Figures 5 and 6, with Table 1 and 2 supporting this non-linear variation.

Conclusions:

Tables 1 and 2 are present new equations for estimating the Young's modulus of CNT-Reinforced Concrete. The models derived exhibited linearity in the elastic limit for all concrete grades and nonlinearity in the elastic tensile strength for any grade of concrete. Finite element modeling revealed that Single-Walled Carbon Nanotubes (SWNTs) provide superior strength enhancement relative to Multi-Walled Carbon Nanotubes (MWNTs). The results corroborate existing research indicating that a larger Carbon Nanotube (CNTs) radius results in a lower effective Young's modulus of CNT composites. The developed finite element model demonstrated convergence at a fiber volume fraction of 0.9%. However, the analytical study may indicate that the concrete strength had minimal impact on the CNTs reinforcement.

These observations indicate that for any concrete grade, this model accurately predicts the transverse moduli of elasticity, given that the fibre volume fraction does not exceed 0.9%. The simulations indicate that preventing the agglomeration of CNTs would result in optimal percentages of CNTs as fiber reinforcements in the derived models. The derived equation, grounded in fundamental material mechanics and corroborated by experimental data, exhibits a significant correlation with observed values. The findings demonstrate that CNT reinforcement increases the stiffness and mechanical properties of concrete, thereby enhancing structural durability and resilience.

Conflict of interest:

The authors declare no conflict of interest.

References:

1. Iijima, S., Synthesis of Carbon Nanotubes. *Nature*, (1991), 354, 56-58. <http://dx.doi.org/10.1038/354056a0>
2. Hasan et al., "Computing the compressive strength of CNT/cement composite," *International Journal of Civil Engineering* (2011), 9(3), 223–229.
3. L. Y. Chan et al., "Mechanical characterization of carbon nanotube reinforced concrete using finite element method."
4. Rouiana et al., "Evaluation of Young's modulus of single walled carbon nanotube reinforced concrete composite," *Journal of Engineering and Applied Sciences*, (2008), 3(6), 504–515.
5. S. I. Yengejeh et al., "Carbon nanotubes as reinforcement in composites: A review of the analytical, numerical and experimental approaches," *Computational Material Science* (2017), 136, 85–101.
6. R. Nadiy, "WS2 nanotube–reinforced cement: Dispersion matters," *Construction and Building Materials* (2015) 98, 112–118.
7. B. M. Tyson et al., "Carbon nanotubes and carbon nanofibers for enhancing the mechanical properties of nanocomposite cementitious materials," *Journal of Materials in Civil Engineering* (2011), 23(7), 1028–1035.
8. Z. Chen et al., "Ultra high performance cement–based composites incorporating low dosage of plasma synthesized carbon nanotubes," *Materials and Design* (2016), 108, 479–487.
9. A. M. Rashad, "Effect of carbon nanotubes (CNTs) on the properties of traditional cementitious Materials," *Construction and Building Materials*, (2017), 153, 81–101.
10. J. F. Wang et al., "A multiscale modeling of CNT–reinforced cement composites,"

- Computer Methods in Applied Mechanics and Engineering, (2016), 309, 411–433.
11. J. F. Wang et al., “Multi scale simulation of mechanical properties and microstructure of CNT–reinforced cement–based composites, (2017),.319, 393–413.
 12. C. Ramesh Babu, “Technical note on using CNTs as reinforcements in reinforced concrete structural elements,” AIP Conference Proceedings, (2017), 1859, 020072.
 13. A. Sza, “Synthesis methods of carbon nanotubes and related materials,” Materials, (2010), 3092–3140.
 14. S. Sasmal and B. Bhuvaneshwari, “Can carbon nanotubes make wonders in civil/structural engineering?,” Progress in Nanotechnology and Nanomaterials, (2013), 2(4), 117–129.
 15. C. Pelissou, “Determination of the size of the representative volume element for random quasi-brittle composites,” International Journal of Solids and Structures, (2009), 46(14-15), 2842–2855.

A Study on the Simplified Equation for the Young's Modulus of Concrete Reinforced Using Carbon Nanotubes (CNT) © 2026 by Nakul Misra is licensed under CC BY 4.0.